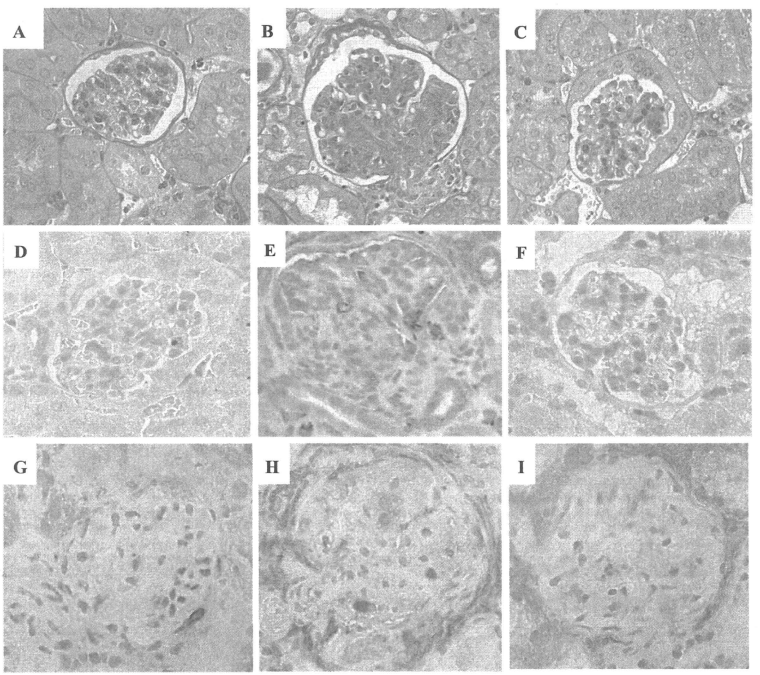

Fig. 1. Representative photomicrographs showing immunohistochemical staining for fractalkine (Fkn) and the presence of CD16+ monocytes (CD16+ Mos) within glomerular lesions in MRL/lpr mice and MRL/Mp+/+ (MRL/+) mice. Periodic acid-Schiff (PAS) staining of glomerular lesions in 4-wk-old MRL/lpr mice (*A*), 20-wk-old MRL/lpr mice (*B*), and 20-wk-old MRL/+ mice (*C*) (magnification, ×400). Fkn (*D–F*) and CD16 (*G–I*) staining in glomerular lesions in 4-wk-old MRL/lpr mice (*D* and *G*), 20-wk-old MRL/lpr mice (*E* and *H*), and 20-wk-old MRL/+ mice (*F* and *I*).

described previously (10). Aliquots (100 μl) of cells (5×10^6/ml) suspended in RPMI 1640–0.5% BSA were added to the upper wells while murine Fkn was added to the lower wells to a final concentration of 5 μg/ml. The cells were then allowed to migrate for 2 h at 37°C in a 5% CO_2 incubator, after which the filters were fixed with 1% glutaraldehyde in PBS for 30 min and stained with 0.5% toluidine blue overnight. Cell migration was quantified by counting the cells in the lower chamber and those adhering to the underside of the polycarbonate filter. In blocking assays, the cells were pretreated with 25 or 50 ng/ml Fkn-AT derived from conditioned medium from L cells transfected with pCXN2 vector carrying the Fkn-AT for 30 min at 37°C before their addition to the upper chambers. As a control, the cells were pretreated with an equivalent volume of conditioned medium from L cells transfected with an empty pCXN2 vector for 30 min at 37°C before their addition to the upper chambers. Each assay was performed in triplicate. Fkn-AT/control pretreated cell migration count ratios were calculated in each concentration of Fkn-AT.

Injection of transfected cells and hybridomas. Transfected L cells (1×10^7 cells) were subcutaneously injected in SCID mice, and 5 days later a hybridoma clone (1×10^7 cells) was injected intraperitoneally. On *day 25* after the first injection, serum samples were collected from the mice under ether anesthesia, and the kidneys, heart, lungs, liver, pancreas, and salivary glands were removed for histopathological examination.

Measurement of Fkn-AT and serum IgG_3, blood urea nitrogen, and albumin using ELISAs. To measure levels of Fkn-AT in culture supernatants conditioned by transfected L cells and in serum of SCID mice injected of transfected L cells, we prepared 96-well Maxisorp plates (Nalge Nunc) containing goat anti-murine Fkn polyclonal antibody. As described previously, the Fkn-AT concentrations in the

serum of Fkn-AT-expressing mice were corrected by subtracting the value obtained in control mice (9). The concentration of IgG_3 in serum was determined using a mouse IgG_3 ELISA Quantitation Kit (Bethyl Laboratories, Montgomery, TX). The concentration of blood urea nitrogen (BUN) and albumin in serum was determined by the Bromcresol green method (Wako Pure Chemical Industries, Osaka, Japan).

Statistical analysis. Numerical results were expressed as means ± SD. Student's paired *t*-test was used for normally distributed variables. When comparing groups, one-way ANOVA was used, followed by post hoc *t*-test with Fisher's protected least significant difference adjustment. For variables having a skewed distribution, we used Kruskal-Wallis ANOVA by ranks, with Bonferroni's adjustment. Values of $P < 0.05$ were considered significant.

RESULTS

Fkn mRNA expression and CD16+ Mos accumulation in the glomeruli of MRL/lpr mice. We found that MRL/lpr mice exhibit progressively worsening renal damage that first became noticeable when the mice were about 12 wk old and that the glomerular lesions exhibited regular variation with progression of the disease. Immunohistochemical and electron microscopic analyses revealed that the lesions were initiated by Ig deposition in the subendothelial, subepithelial, and mesangial regions, which was followed by segmental mesangial proliferation. At age 4 wk, glomeruli remained nearly intact or showed slight mesangial proliferation. By 20 wk, however, endocapillary proliferative lesions characteristic of severe inflammatory cell infiltration had formed, causing the glomeruli to assume a lobular structure that was associated with segmental lesions with wire-loop and/or hyaline thrombus formation (Fig. 1).

We initially used immunohistochemistry to analyze glomerular Fkn expression and CD16+ Mos accumulation and found that there was a significant increase in both glomerular Fkn expression and CD16+ Mos accumulation in MRL/lpr mice by the time they were 20 wk old (Fig. 1). We then carried out real-time PCR using glomerular RNA collected by LCM to analyze glomerular Fkn transcription in 4- and 20-wk-old MRL/lpr mice and 20-wk-old MRL/+ mice. In addition, we also obtained the corresponding glomerular CD16+ Mo counts. We found that, in MRL/lpr mice, both the glomerular Fkn mRNA expression and the CD16+ Mo counts were significantly ($P < 0.01$) higher at age 20 wk (Fig. 2) than at age 4 wk, suggesting glomerular Fkn expression and CD16+ Mos infiltration increases with progression of the lupus nephritis in MRL/lpr mice. By contrast, the glomeruli of 20-wk-old MRL/+ mice showed no abnormalities, with no detectable glomerular Fkn expression or CD16+ Mos accumulation (Figs. 1 and 2).

Fkn mRNA expression and CD16+ Mos accumulation in two types of glomerular lesions induced by monoclonal antibodies. In SCID lupus model mice, injection of 2B11.3 and 7B6.8 clones, respectively, induced endocapillary proliferative and wire-loop glomerular lesions within 15–25 days after injection, as reported previously (Fig. 3) (21). Notably, the clone-induced lesions reflected the complex histopathology of glomerular lesions seen in 20-wk-old MRL/lpr mice, which are characterized by endocapillary proliferative lesions segmentally associated with wire-loop and hyaline thrombotic lesions. By contrast, the 1G3 clone, used as a control IgG_3 antibody, did not induce significant glomerular lesions (Fig. 3), although there were no significant differences in serum IgG_3 levels among the three groups (2B11.3, 7B6.8, and 1G3: 1.22 ± 0.31, 1.19 ± 0.36, and 1.52 ± 0.41 mg/ml).

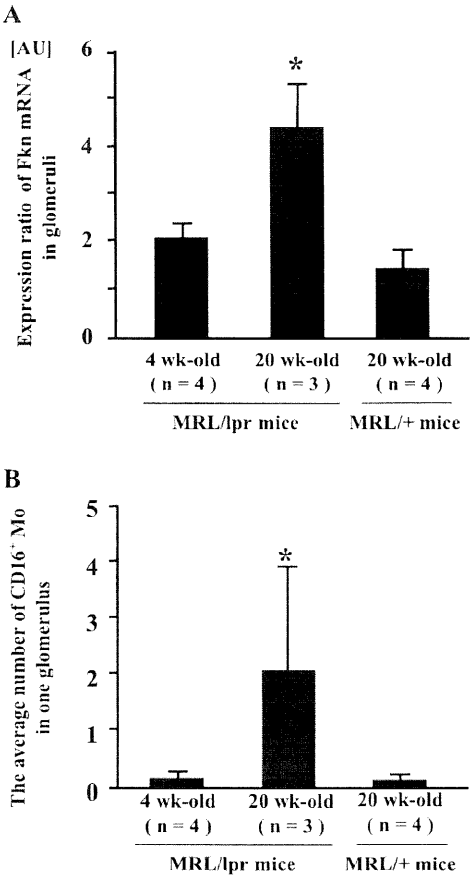

Fig. 2. Fkn mRNA levels and CD16+ Mos counts in glomeruli of 4-wk-old MRL/lpr mice, 20-wk-old MRL/lpr mice, and 20-wk-old MRL/+ mice. *A*: Fkn mRNA levels in arbitrary units. *B*: average no. of immunohistochemically identified CD16+ Mos within the glomeruli of 4-wk-old MRL/lpr mice (n = 4), 20-wk-old MRL/lpr mice (n = 3), and 20-wk-old MRL/+ mice (n = 4). Kruskal-Wallis ANOVA by ranks with Bonferroni's adjustment was used for comparison between groups. Bars depict means ± SE. *$P < 0.01$ vs. 4-wk-old MRL/lpr mice and 20-wk-old MRL/+ mice.

Serum BUN levels were markedly elevated in mice injected with 2B11.3 or 7B6.8 clone (72.3 ± 30.5 mg/dl, n = 7, $P < 0.05$ and 68.4 ± 32.4 mg/dl, n = 5, $P < 0.05$, respectively) compared with those injected with 1G3 clone (22.6 ± 7.5 mg/dl, n = 4). There was no significant difference in serum BUN levels (P = 0.83) between mice injected with 2B11.3 clone and those injected with 7B6.8 clone. Moreover, there was a marked reduction in serum albumin levels in mice injected with 2B11.3 or 7B6.8 clone (1.7 ± 0.9 mg/dl, n = 7, $P < 0.05$ and 1.8 ± 0.7 mg/dl, n = 5, $P < 0.05$, respectively) compared with those injected with 1G3 clone (3.4 ± 0.5 mg/dl, n = 4). Again, there was no significant difference in serum albumin levels between mice injected with 2B11.3 clone and those injected with 7B6.8 clone (P = 0.84).

In a second set of experiments, we analyzed the relationship between levels of Fkn expression and the histopathology of these monoclonal antibody-induced glomerular lesions in

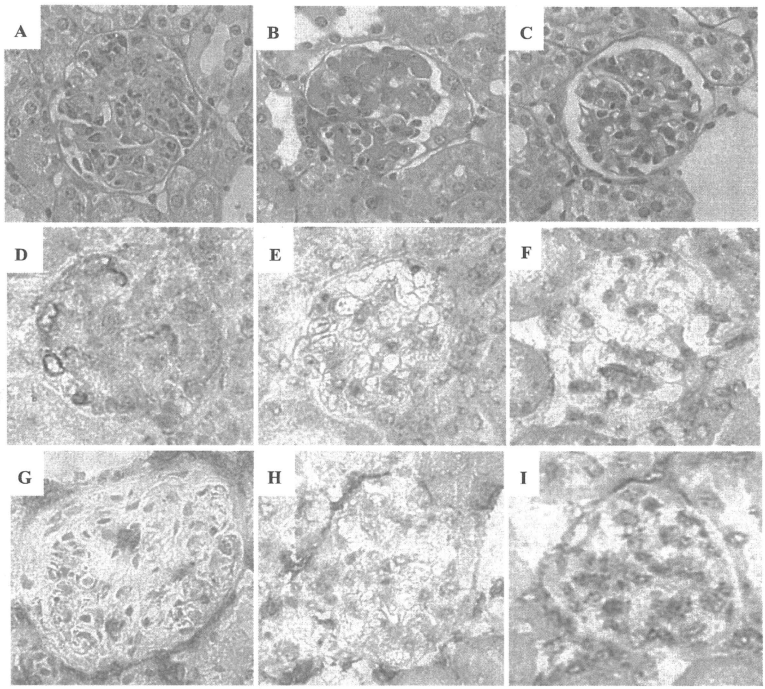

Fig. 3. Representative photomicrographs and immunohistochemical staining for Fkn and CD16+ Mos within glomerular lesions in C.B-17/Inc-scid/scid (SCID) lupus model mice injected with IgG_3-producing hybridomas. PAS staining of proliferative glomerular lesions induced by clone 2B11.3 (*A*), wire-loop-like glomerular lesions induced by clone 7B6.8 (*B*), and a normal glomerulus in a mouse administered clone 1G3 (*C*) (magnification, ×400). Fkn (*D–F*) and CD16 (*G–I*) staining in glomerular lesions induced by clones 2B11.3 (*D* and *G*) and 7B6.8 (*E* and *H*) and in control glomeruli from a mouse administered clone 1G3 (*F* and *I*).

SCID mice. In the glomerular lesions induced by 2B11.3, Fkn expression was detected in mesangial areas and along capillary walls, whereas it was not detected in glomerular lesions induced by 7B6.8 or 1G3 (Fig. 3). 2B11.3 clone also induced significantly ($P < 0.005$) greater expression of Fkn mRNA in glomerular lesions than did 7B6.8 or 1G3 clone (Fig. 4*A*). Likewise, CD16+ Mo counts were significantly ($P < 0.001$) higher in glomerular lesions induced by 2B11.3 clone than in those induced by 7B6.8 or 1G3 clone (Figs. 3 and 4*B*).

We defined the predisease glomeruli in SCID mice injected with 2B11.3 clone as containing few infiltrating inflammatory cells, despite deposition of IgG_3 in mesangial areas and along capillary walls (Fig. 5, *A* and *B*). At the predisease stage, serum BUN and albumin levels were normal (BUN and albumin: 25.4 ± 8.7 and 3.0 ± 0.8 mg/dl, $n = 7$) in SCID mice injected with 2B11.3 clone. Immunohistochemical analysis revealed no expression of Fkn protein in predisease glomeruli (Fig. 5*C*), and Fkn mRNA levels were about the same as in glomeruli from control mice (Fig. 4*A*). On the other hand, glomerular expression of the proinflammatory cytokines TNF-α and IL-1β was significantly higher in predisease glomeruli than in normal glomeruli, although not as high as in the diseased glomeruli (Fig. 5*D*). Thus Fkn expression was not substantially increased in predisease glomeruli in SCID mice injected with 2B11.3 clone. Levels of TNF-α and IL-1β mRNA were slightly higher in glomerular lesions induced by 7B6.8 clone than in glomeruli from control mice, but the difference was not significant (TNF-α: $P = 0.188$, IL-1β: $P = 0.078$) (Fig. 5*D*).

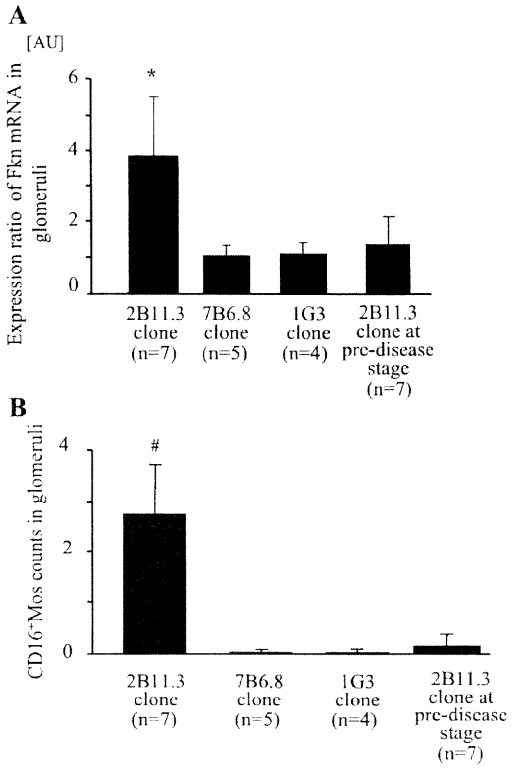

Fig. 4. Fkn mRNA levels and CD16+ Mos counts in glomeruli from SCID mice injected with IgG_3-producing hybridomas. *A*: Fkn mRNA levels in arbitrary units. *B*: average no. of immunohistochemically identified CD16+ Mos in glomeruli from diseased mice administered clone 2B11.3 (n = 7), 7B6.8 (n = 5), or 1G3 (n = 4) or mice at a predisease stage after administration of clone 2B11.3 (n = 7). Kruskal-Wallis ANOVA by ranks with Bonferroni's adjustment was used for comparison between groups. Bars depict means ± SE. *P < 0.005 vs. 7B6.8 clone, 1G3 clone, and 2B11.3 clone at the predisease stage. #P < 0.001 vs. clone 7B6.8, clone 1G3, and clone 2B11.3 at the predisease stage.

Fkn mRNA expression induced in HUVECs and murine MCs by combined stimulation with TNF-α and IL-1β. We next examined the effects of TNF-α and IL-1β on expression of Fkn mRNA in HUVECs and murine MCs. Addition of TNF-α plus IL-1β to HUVEC cultures strongly and dose-dependently increased expression of Fkn mRNA within 6 h (Fig. 6, *A* and *B*) and had a similar effect in murine MCs (Fig. 6, *C* and *D*). This suggests that Fkn expression is likely induced in glomerular endothelial and MCs in response to combined stimulation by TNF-α and IL-1β.

Production of Fkn-AT in SCID mice. In this study, we prepared L cell transfectants that expressed and secreted Fkn-AT (Fig. 7*A*) that significantly inhibited Fkn-stimulated chemotaxis of murine spleen cells (Fig. 7*C*). When L cells were injected in SCID mice, those receiving Fkn-AT-producing cells showed high serum levels of Fkn-AT by *day 25* after injection while those receiving control L cells did not (Fig. 7*B*).

Effect of Fkn-AT on glomerular lesions in SCID mice injected with 2B11.3 clone. The proliferative glomerular lesions in SCID mice injected with 2B11.3 clone appeared to be significantly less severe in mice pretreated with Fkn-AT-producing L cells than in those pretreated with control cells [Fkn-AT and control (index of glomerular lesions): 1.25 ± 0.12 and 2.54 ± 0.29 (P < 0.01) (Fig. 8, *A*, *B*, and *G*)]. In addition, there was a significant (P < 0.01) reduction in glomerular infiltration by CD16+ Mos in mice treated with Fkn-AT-producing L cells compared with control (Fkn-AT vs. control: 0.13 ± 0.03 vs. 0.66 ± 0.29, P < 0.05) (Fig. 8, *C*, *D*, and *H*). Moreover, the elevation of serum BUN and hypoalbuminemia was strongly inhibited in mice pretreated with Fkn-AT-producing L cells compared with control (Fkn-AT vs. control: BUN, 35.3 ± 2.9 vs. 58.8 ± 11.6 mg/dl; Alb, 3.01 ± 0.33 vs. 1.75 ± 0.24 mg/dl; n = 5, P < 0.05). On the other hand, when SCID mice were pretreated with Fkn-AT-producing L cells, glomerular wire-loop lesions in mice injected with 7B6.8 clone showed no significant change from control [Supplemental Fig. 1, *A* and *B* (Supplemental data for this article can be found on the *American Journal of Physiology: Renal Physiology* website.)]. Likewise, serum BUN and albumin levels in mice pretreated with Fkn-AT-producing L cells did not significantly differ from control (Fkn-AT vs. control: BUN, 55.9 ± 11.5 vs. 58.2 ± 11.4 mg/dl, P = 0.76; albumin, 1.83 ± 0.27 vs. 1.57 ± 0.23 mg/dl, P = 0.13).

The glomerular deposition of IgG_3 in mice injected with Fkn-AT-producing L cells and those injected with control L cells appeared similar when the mice were injected with 2B11.3 clone (Fig. 8, *E* and *F*) or 7B6.8 clone (Supplemental Fig. 1, *E* and *F*). No IgG_3 was detected elsewhere in the kidney, nor was any detected in the lung or liver. Moreover, there was no significant difference in serum IgG_3 levels between mice injected with Fkn-AT-producing cells and those injected with control cells (2B11.3 clone: Fkn-AT vs. control, 0.72 ± 0.31 vs. 0.78 ± 0.38 mg/ml; 7B6.8 clone: Fkn-AT vs. control, 0.81 ± 0.42 vs. 0.84 ± 0.34 mg/ml).

DISCUSSION

In this study, we demonstrated Fkn expression and CD16+ Mos accumulation within proliferative glomerular lesions, but not in wire-loop-like lesions, in SCID lupus model mice injected with IgG_3-producing hybridoma clones derived from an MRL/lpr mouse. In addition, we found that Fkn-AT mitigated the progression of proliferative glomerular lesions as well as glomerular infiltration by CD16+ Mos in these mice.

Fkn is a mononuclear cell-directed, cell surface-anchored chemokine that likely plays an essential role in the recruitment and accumulation of CX3CR1-expressing leukocytes, especially monocytes/macrophages, under conditions of high blood flow like that in glomerular capillaries (7, 12). CD16+ Mos are thought to express higher levels of CX3CR1 than CD16− Mos and to also produce high levels of proinflammatory cytokines (2, 8, 27). We previously reported that both Fkn expression and CD16+ Mos accumulation are markedly elevated in patients with proliferative lupus nephritis (ISN/RPS classes III and IV) (26), but it remained uncertain whether Fkn played any significant role in the pathogenesis of glomerular lesions in lupus nephritis. For that reason, our first set of experiments was undertaken to assess the degree to which the level of Fkn expression in glomeruli was related to the severity of glomerular lesions in MRL/lpr mice, which are regarded as a good model of proliferative lupus nephritis. An earlier study showed

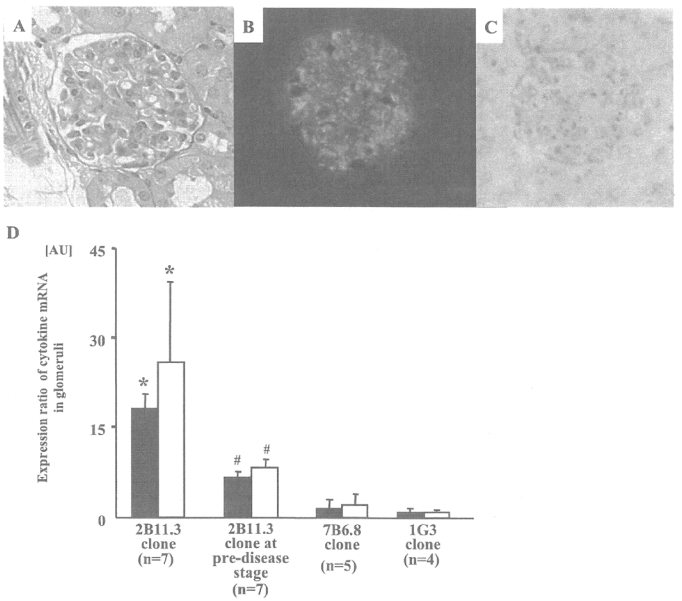

Fig. 5. Representative photomicrographs of glomerular lesions and immunofluorescent staining for IgG_3 and Fkn in SCID mice at the predisease stage after injection with clone 2B11.3 and levels of proinflammatory cytokine mRNAs in glomeruli of SCID mice injected with IgG_3-producing hybridomas. PAS staining (*A*) (magnification, ×400) and immunofluorescent staining with anti-IgG_3 (*B*) or anti-Fkn (*C*) in glomerular lesions in SCID mice at a predisease stage after injection with 2B11.3 clone. *D*: expression of tumor necrosis factor (TNF)-α (filled bars) and interleukin (IL)-1β (open bars) mRNA induced in glomeruli by 2B11.3 clone (n = 7), 2B11.3 clone at a predisease stage (n = 7), 7B6.8 clone (n = 5), and 1G3 clone (n = 4). Kruskal-Wallis ANOVA by ranks with Bonferroni's adjustment was used for comparison between groups. Bars depict means ± SE in arbitrary units. *$P < 0.005$ vs. 2B11.3 clone at a predisease stage and 1G3 clone. #$P < 0.05$ vs. 1G3 clone.

that renal expression of Fkn was upregulated in MRL/lpr mice during the development of renal damage (13), but the relation between the severity of the glomerular lesions and the level of Fkn expression was unclear. We therefore semiquantitatively analyzed expression of Fkn mRNA in glomeruli using LCM, which enabled us to rapidly isolate selected glomeruli from MRL/lpr mice, based on the degree of injury. We found significant levels of Fkn expression and CD16$^+$ Mos accumulation in the glomeruli of 20-wk-old MRL/lpr mice, suggesting that Fkn expression and CD16$^+$ Mos accumulation contribute to the progression of glomerular lesions in these animals. However, glomerular lesions of 20-wk-old MRL/lpr mice were histopathologically very heterogeneous, and it is unclear which glomerular lesions of MRL/lpr mice are actually associated with Fkn expression and CD16$^+$ Mos accumulation.

Our second set of experiments was undertaken to further clarify the association between Fkn expression with the observed diversity of glomerular lesions using a simplified lupus nephritis model in which glomerular lesions were induced with monoclonal antibodies derived from an MRL/lpr mouse. In SCID mice injected with IgG_3-producing hybridoma clones, both Fkn expression and CD16$^+$ Mo counts were markedly elevated in endocapillary proliferative glomerular lesions, but not in wire-loop lesions. This may mean that the histopathological variation in glomerular lesions seen in MRL/lpr mice is a reflection of the expanded B cell clones and the pathogenic potencies of different antibodies they express.

To determine whether the observed increase in Fkn expression was a cause or a result of inflammatory cell infiltration in the glomeruli of SCID mice injected with IgG_3-producing hybridoma clone 2B11.3; we also evaluated glomerular Fkn expression at a predisease stage, during which glomerular deposition of IgG_3 was detected, but inflammatory cells and/or proliferative lesion were not. We found that Fkn expression was not yet upregulated in

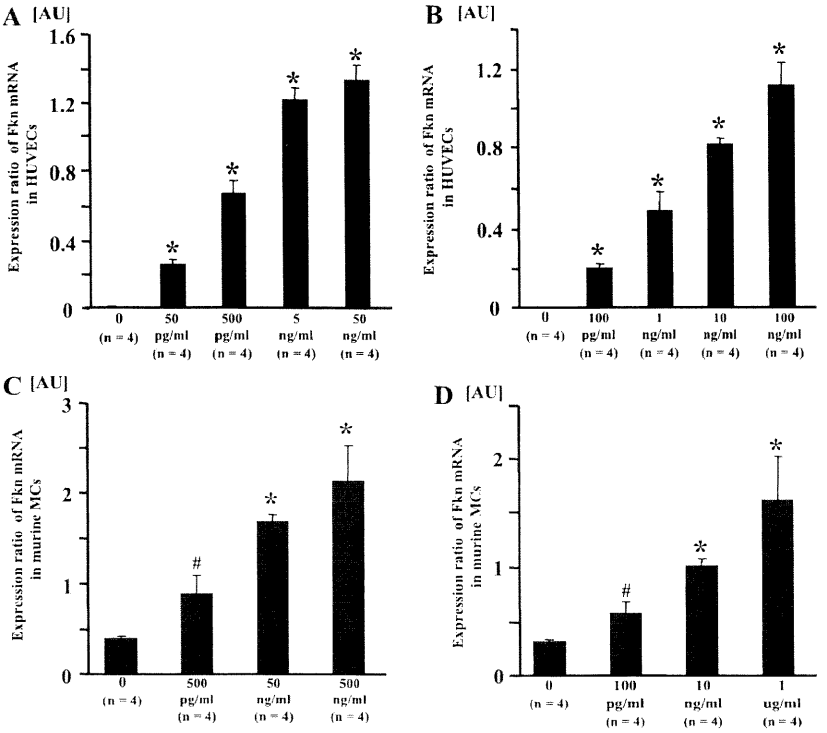

Fig. 6. Effects of cytokines on expression of Fkn mRNA. Expression of Fkn mRNA levels in human umbilical vein endothelial cells (HUVECs) (*A* and *B*) and murine mesangial cells (MCs) (*C* and *D*) induced by the combination of TNF-α (*A* and *C*) and IL-1β (*B* and *D*) at the indicated concentrations. Bars depict means ± SE in arbitrary units. *$P < 0.001$ vs. 0 pg/ml. #$P < 0.01$ vs. 0 pg/ml.

endocapillary proliferative glomerular lesions at the predisease stage, but levels of two proinflammatory cytokines, TNF-α and IL-1β, were already elevated. By contrast, levels of these two proinflammatory cytokines were not significantly elevated in the glomeruli of SCID mice injected with 7B6.8 clone. In vitro, Fkn mRNA expression in HUVECs and MCs increased in response to combined stimulation with TNF-α and IL-1β; moreover, we recently observed that 2B11.3 antibodies do not induce Fkn expression by cultured endothelial cells (data not shown). Taken together, these findings suggest that Fkn expression is induced in response to the production of inflammatory cytokines such as TNF-α and IL-1β triggered by complement activation and/or accumulation of circulating leukocytes in the glomeruli of SCID mice injected with 2B11.3 clone and that it is not primarily induced by the deposition of 2B11.3 antibodies. Inflammatory cytokines released from infiltrating leukocytes may induce Fkn

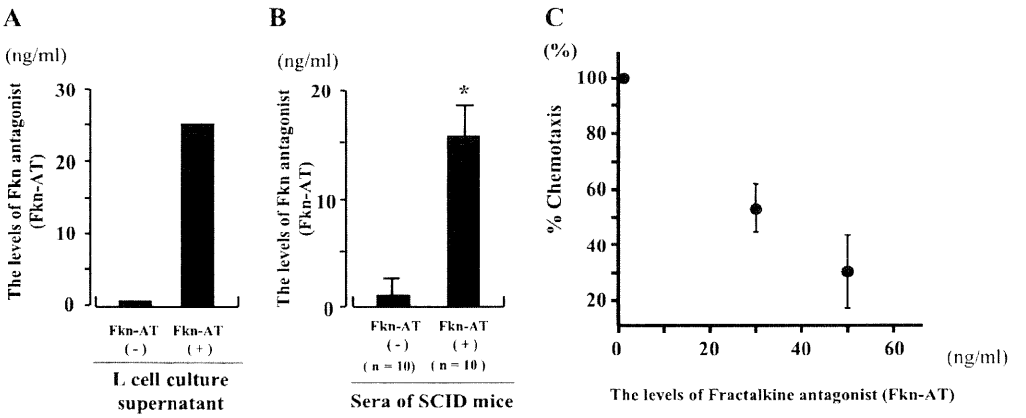

Fig. 7. ELISAs of Fkn antagonist (Fkn-AT) and inhibition of chemotaxis. *A*: levels of Fkn-AT in L cell culture supernatant. *B*: levels of Fkn-AT in serum from SCID mice collected 25 days after injection with L cells ($n = 5$). *C*: inhibition of murine spleen cell chemotaxis by Fkn-AT produced by L cells. Chemotaxis was assayed after murine spleen cells were pretreated with the indicated concentration of Fkn-AT for 30 min at 37°C. Experiments were performed in triplicate. Values are means ± SD; bars depict means ± SE. *$P < 0.005$ vs. control L cells.

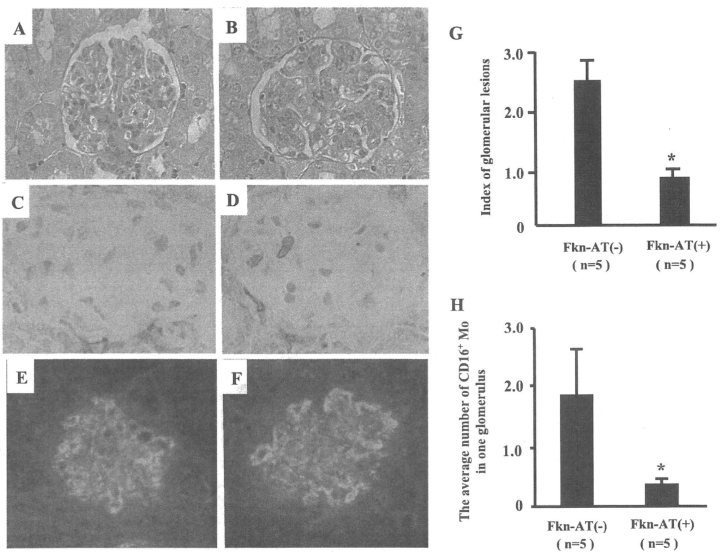

Fig. 8. Representative photomicrographs of glomerular lesions and $CD16^+$ Mos counts in SCID mice bearing L cells 20 days after injection of clone 2B11.3. *A*: PAS staining (*A* and *B*) (magnification, ×400) and CD16 (*C* and *D*) and IgG_3 (*E* and *F*) staining within glomerular lesions in SCID mice bearing Fkn-AT-producing L cells (*A*, *C*, and *E*) or control L cells (*B*, *D*, and *F*) 20 days after injection of clone 2B11.3. *G*: index of glomerular lesions. *H*: average no. of immunohistochemically identified $CD16^+$ Mos in glomerular lesions induced by clone 2B11.3 in SCID mice (n = 5). Unpaired 2-tailed Student's t-test was used for comparison between groups. Bars depict means ± SE. $*P < 0.01$ vs. control L cells.

expression to accelerate further accumulation of leukocytes, such as $CD16^+$ Mos, thereby exacerbating the proliferative glomerular lesions of lupus nephritis.

These findings prompted us to speculate that we could mitigate the proliferative glomerular lesions in this lupus model mouse by using an Fkn-AT to reduce the infiltration of inflammatory cells such as $CD16^+$ Mos. To test that idea, we developed a system to overproduce Fkn-AT in the circulation by transplanting Fkn-AT-producing L cells in SCID mice. The antagonist consisted of an Fkn truncation mutant in which the four NH_2-terminal amino acid residues were removed. This molecule was previously shown to be a potent Fkn-AT and to ameliorate the progression of lupus nephritis in MRL/lpr mice (10). We found that Fkn-AT protected against the development of glomerular endocapillary proliferative lesions induced by clone 2B11.3 in SCID mice while markedly reducing glomerular $CD16^+$ Mos accumulation. However, Fkn-AT did not protect against the development of glomerular wire-loop lesions induced by 7B6.8 clone. It thus appears that, by stimulating $CD16^+$ Mos accumulation, Fkn contributes to the development of endocapillary proliferative glomerular lesions induced by monoclonal antibodies raised in SCID mice, which completely lack T and B cells but have a normal granulomonocyte system. That said, other pathways that do not involve Fkn-$CD16^+$ Mos interaction may also contribute to lupus nephritis, for example, glomerular wire-loop lesions induced by clone 7B6.8. Further study will be needed to clarify these pathways with the goal of complete amelioration of lupus nephritis.

In conclusion, Fkn expression and $CD16^+$ Mos accumulation in glomeruli is associated with the histopathology of glomerular lesions in MRL/lpr mice. Fkn appears to mainly affect the progression of proliferative glomerular lesions of lupus nephritis and does not trigger lesion formation. Fkn-AT may thus represent potentially useful tools for targeting leukocytes such as $CD16^+$ Mos, which mediate the glomerular injury seen in lupus nephritis.

ACKNOWLEDGMENTS

We are indebted to Aya Asano, Hiromi Ohura, and Miyako Sakaida of Nara Medical University for excellent technical assistance.

DISCLOSURES

No conflicts of interest, financial or otherwise, are declared by the authors.

REFERENCES

1. **Ancuta P, Moses A, Gabuzda D.** Transendothelial migration of CD16+ monocytes in response to fractalkine under constitutive and inflammatory conditions. *Immunobiology* 209: 11–20, 2004.
2. **Ancuta P, Rao R, Moses A, Mehle A, Shaw SK, Luscinskas FW, Gabuzda D.** Fractalkine preferentially mediates arrest and migration of CD16+ monocytes. *J Exp Med* 197: 1701–1707, 2003.
3. **Andrews BS, Eisenberg RA, Theofilopoulos AN, Izui S, Wilson CB, McConahey PJ, Murphy ED, Roths JB, Dixon FJ.** Spontaneous murine lupus-like syndromes. Clinical and immunopathological manifestations in several strains. *J Exp Med* 148: 1198–1215, 1978.
4. **Bazan JF, Bacon KB, Hardiman G, Wang W, Soo K, Rossi D, Greaves DR, Zlotnik A, Schall TJ.** A new class of membrane-bound chemokine with a CX3C motif. *Nature* 385: 640–644, 1997.
5. **Cameron JS.** Lupus nephritis. *J Am Soc Nephrol* 10: 413–424, 1999.
6. **Ebling F, Hahn BH.** Restricted subpopulations of DNA antibodies in kidneys of mice with systemic lupus. Comparison of antibodies in serum and renal eluates. *Arthritis Rheum* 23: 392–403, 1980.
7. **Fong AM, Robinson LA, Steeber DA, Tedder TF, Yoshie O, Imai T, Patel DD.** Fractalkine and CX3CR1 mediate a novel mechanism of leukocyte capture, firm adhesion, and activation under physiologic flow. *J Exp Med* 188: 1413–1419, 1998.
8. **Geissmann F, Jung S, Littman DR.** Blood monocytes consist of two principal subsets with distinct migratory properties. *Immunity* 19: 71–82, 2003.
9. **Hasegawa H, Kohno M, Sasaki M, Inoue A, Ito MR, Terada M, Hieshima K, Maruyama H, Miyazaki J, Yoshie O, Nose M, Fujita S.** Antagonist of monocyte chemoattractant protein 1 ameliorates the initiation and progression of lupus nephritis and renal vasculitis in MRL/lpr mice. *Arthritis Rheum* 48: 2555–2566, 2003.
10. **Hasegawa H, Nomura T, Kohno M, Tateishi N, Suzuki Y, Maeda N, Fujisawa R, Yoshie O, Fujita S.** Increased chemokine receptor CCR7/EBI1 expression enhances the infiltration of lymphoid organs by adult T-cell leukemia cells. *Blood* 95: 30–38, 2000.
11. **Hasegawa H, Utsunomiya Y, Kishimoto K, Yanagisawa K, Fujita S.** SFA-1, a novel cellular gene induced by human T-cell leukemia virus type 1, is a member of the transmembrane 4 superfamily. *J Virol* 70: 3258–3263, 1996.
12. **Imai T, Hieshima K, Haskell C, Baba M, Nagira M, Nishimura M, Kakizaki M, Takagi S, Nomiyama H, Schall TJ, Yoshie O.** Identification and molecular characterization of fractalkine receptor CX3CR1, which mediates both leukocyte migration and adhesion. *Cell* 91: 521–530, 1997.
13. **Inoue A, Hasegawa H, Kohno M, Ito MR, Terada M, Imai T, Yoshie O, Nose M, Fujita S.** Antagonist of fractalkine (CX3CL1) delays the initiation and ameliorates the progression of lupus nephritis in MRL/lpr mice. *Arthritis Rheum* 52: 1522–1533, 2005.
14. **Itoh J, Nose M, Takahashi S, Ono M, Terasaki S, Kondoh E, Kyogoku M.** Induction of different types of glomerulonephritis by monoclonal antibodies derived from an MRL/lpr lupus mouse. *Am J Pathol* 143: 1436–1443, 1993.
15. **Iwano M, Dohi K, Hirata E, Horii Y, Shiiki H, Ishikawa H.** Induction of interleukin 6 synthesis in mouse glomeruli and cultured mesangial cells. *Nephron* 62: 58–65, 1992.
16. **Izui S, McConahey PJ, Theofilopoulos AN, Dixon FJ.** Association of circulating retroviral gp70-anti-gp70 immune complexes with murine systemic lupus erythematosus. *J Exp Med* 149: 1099–1116, 1979.
17. **Kotzin BL.** Systemic lupus erythematosus. *Cell* 85: 303–306, 1996.
18. **May LT, Sehgal PB.** On the relationship between human interferon alpha 1 and beta 1 genes. *J Interferon Res* 5: 521–526, 1985.
19. **Mikulowska-Mennis A, Taylor TB, Vishnu P, Michie SA, Raja R, Horner N, Kunitake ST.** High-quality RNA from cells isolated by laser capture microdissection. *Biotechniques* 33: 176–179, 2002.
20. **Murphy ED, Roths JB.** *Autoimmunity and Lymphoprokiferation: Induction by Mutant Gene lpr, and Acceleration by a Male-Associated Factor in Strain BXSB Mice.* New York, NY: Elsevier North Holland; 1979.
21. **Nakatani K, Fujii H, Hasegawa H, Terada M, Arita N, Ito MR, Ono M, Takahashi S, Saiga K, Yoshimoto S, Iwano M, Shiiki H, Saito Y, Nose M.** Endothelial adhesion molecules in glomerular lesions: association with their severity and diversity in lupus models. *Kidney Int* 65: 1290–1300, 2004.
22. **Nardella FA, Teller DC, Izui S, Mannik M.** Self-associating IgG rheumatoid factors in MRL/l autoimmune mice. *Arthritis Rheum* 27: 1165–1173, 1984.
23. **Rossi DL, Hardiman G, Copeland NG, Gilbert DJ, Jenkins N, Zlotnik A, Bazan JF.** Cloning and characterization of a new type of mouse chemokine. *Genomics* 47: 163–170, 1998.
24. **Tadros Y, Ruiz-Deya G, Crawford BE, Thomas R, Abdel-Mageed AB.** In vivo proteomic analysis of cytokine expression in laser capture-microdissected urothelial cells of obstructed ureteropelvic junction procured by laparoscopic dismembered pyeloplasty. *J Endourol* 17: 333–336, 2003.
25. **Takahashi S, Nose M, Sasaki J, Yamamoto T, Kyogoku M.** IgG3 production in MRL/lpr mice is responsible for development of lupus nephritis. *J Immunol* 147: 515–519, 1991.
26. **Yoshimoto S, Nakatani K, Iwano M, Asai O, Samejima K, Sakan H, Terada M, Harada K, Akai Y, Shiiki H, Nose M, Saito Y.** Elevated levels of fractalkine expression and accumulation of CD16+ monocytes in glomeruli of active lupus nephritis. *Am J Kidney Dis* 50: 47–58, 2007.
27. **Ziegler-Heitbrock HW.** Heterogeneity of human blood monocytes: the CD14+ CD16+ subpopulation. *Immunol Today* 17: 424–428, 1996.

Clinical Nephrology, Vol. 74 – No. 5/2010 (384-388)

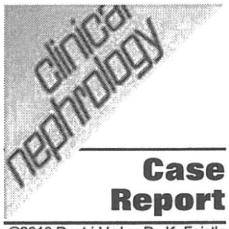

Case Report

ISSN 0301-0430

DOI 10.2379/CNX06365

Resolution of mesangial light chain deposits 3 years after high-dose melphalan with autologous peripheral blood stem cell transplantation

K. Harada, Y. Akai, H. Sakan, Y. Yamaguchi, K. Nakatani, M. Iwano and Y. Saito

First Department of Internal Medicine, Nara Medical University, Nara, Japan

Key words
light chain deposition disease – multiple myeloma – remission – nodular lesion

Abstract. A 52-year-old woman was admitted to our hospital for treatment of nephrotic syndrome. Funduscopic findings showed fundal hemorrhage and soft exudates, and serologic analysis showed a monoclonal serum component that was identified as Bence Jones protein-κ type. A bone marrow biopsy showed diffuse proliferation of atypical plasma cells, while a renal biopsy showed diffuse and nodular mesangial proliferation. Immunohistochemical staining confirmed the presence of κ chains along the glomerular basement membrane and in mesangial areas. The patient was diagnosed as multiple myeloma (Bence Jones κ type) with light chain deposition disease (LCDD). After high-dose melphalan and autologous peripheral blood stem cell transplantation (PBSCT), the multiple myeloma and nephrotic syndrome were in complete remission; her renal function was improved, but a renal biopsy performed 6 months after PBSCT showed the persistence of diffuse and nodular lesions. By contrast, a renal biopsy performed 3 years later showed complete resolution of the diffuse and nodular mesangial proliferation.

Introduction

Nonamyloidotic monoclonal immunoglobulin deposition disease (MIDD) is characterized by nodular sclerosing glomerulopathy, proteinuria, renal insufficiency, and an association with dysproteinemias [1]. Histological evaluation reveals monoclonal light and/or heavy chain deposits within the basement membranes of glomeruli, tubules and vessels. One type of MIDD, light chain deposition disease (LCDD), is the most prevalent and was detected in 19% of 118 renal biopsies from patients with multiple myeloma (MM) [12]. However, there have been few reports of renal histology performed after remission of MM. In the present report, we describe a case of MM with LCDD in which a follow-up renal biopsy after the patient had been in remission for 3 years showed remarkable histological resolution.

Case report

A 52-year-old Japanese female patient was admitted to our hospital in May, 2004 with nephrotic syndrome. She had been diagnosed with hypertension and nephrotic syndrome in January, 2004. At that time she was exhibiting anasarca, as antihypertensive agents and diuretics were ineffective. She worked in an office, was a non-smoker, drank alcohol socially and had no history of illicit/recreational drug use. Her family history was negative for hematological malignancy or gastrointestinal disease.

On admission the patient was afebrile and hypertensive (160/90 mmHg), with a pulse of 86 beats/min. She had scleral anemia, and funduscopic findings showed fundal hemorrhage and soft exudates. Her cervical, axillary, and inguinal lymph nodes were not palpable. Her chest was clear on auscultation, and cardiac sounds were normal, without gallop or murmur. She had 2 – 3+ pitting edema in the bilateral lower extremities. Her skin was moist, and there was no joint or soft tissue swelling, tenderness or deformity. Neurological examination was unremarkable. Her complete blood count was also normal, but she showed hypoproteinemia with both hypoalbuminemia and hypogammaglobulinemia. 24-h urinary protein was 4.8 g, serum cre-

Received
January 23, 2009;
accepted in revised form
August 18, 2009

Correspondence to
M. Iwano, MD
First Department of
Internal Medicine,
Nara Medical University,
840 Shijo, Kashihara,
Nara 634-8522 Japan
miwano@
naramed-u.ac.jp

Table 1. Laboratory data on admission.

Urinalysis		LDH	249 IU/l
Protein	4.8 g/day	Transferrin saturation	19.8 %
Glucose	(–)	Ferritin	167 ng/ml
Red blood cells	10 – 19/HPF	Sodium	149 mEq/l
White blood cells	20 – 29/HPF	Potassium	3.8 mEq/l
		Chloride	114 mEq/l
Hematology		Calcium	8.8 mg/dl
Red blood cells	301×10^4 μl	Phosphate	4.5 mg/dl
Hemoglobin	9.6 g/dl		
Hematocrit	28.4%		
White blood cells	4,700/μl	Serology	
Neutrophils	54.0%	CRP	0.5 mg/dl
Monocytes	6.0%	Antinuclear antibodies	(–)
Lymphocytes	32.0%	IgG	297 mg/dl
Platelet	23.3×10^4 μl	IgA	40.4 mg/dl
		IgM	10.8 mg/dl
Erythrocyte sedimentation rate		CH50	41 U/ml
	100 mm/1 h	C3	126 mg/dl
Chemistry		C4	56.0 mg/dl
Total protein	5.0 g/dl	Immune complex	(–)
Albumin	3.1 g/dl	Cryoglobulins	(–)
Total cholesterol	223 mg/dl	M protein	(+)
Creatinine	1.5 mg/dl		
Blood urea nitrogen	20 mg/dl	Immunoelectrophoresis	
Uric acid	5.9 mg/dl	BJP	κ type
Total bilirubin	0.6 mg/dl		
AST	14 IU/dl	Renal function test	
ALT	13 IU/l	Creatinine clearance	41.4 ml/minute

tinine concentration and 24-h creatinine clearance were 1.5 mg/dl and 41.4 ml/min, respectively. Serologic analysis revealed monoclonal gammanopathy, the monoclonal component being Bence Jones protein-κ type (Table 1). A bone marrow biopsy showed the proportion of atypical plasma cells to be 42.4%. A renal biopsy performed to differentiate the nephrotic syndrome revealed diffuse and nodular mesangial proliferation and mild endocapillary proliferation (Figure 1A). Immunohistochemical staining confirmed the presence of κ chains along the glomerular membrane and in mesangial areas (Figure 1B). The patient was diagnosed as having MM (Bence Jones κ type) with LCDD.

She was treated with 2 courses of VAD (vincristine 0.4 mg/day, adriamycin 10 mg/day, and dexamethasone 40 mg/day), followed by high-dose chemotherapy with melphalan 120 mg/day. After the chemotherapy, the patient required autologous peripheral blood stem cell transplantation (PBSCT), followed by oral thalidomide 200 mg/day, and the MM and nephrotic syndrome were in complete remission. A renal biopsy performed 6 months later showed diminished endocapillary proliferation, but the diffuse and nodular mesangial proliferation persisted (Figure 1C,D). A renal biopsy performed after 3 years of remission showed marked resolution of the nodular mesangial proliferation (Figure 1E,F). Elec-

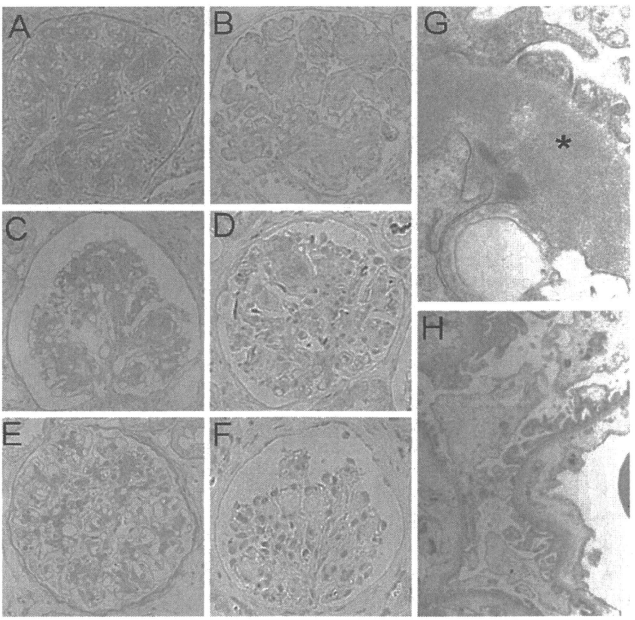

Figure 1. Findings in the renal biopsy specimens. In the initial renal biopsy, periodic acid-Schiff (PAS)-positive nodules and homogenous depositions of κ light-chain were observed in light microscopy (A) and immunohistochemistry (B). These lesions were still found in the second biopsy (C, D), but disappeared almost completely in the third biopsy (E, F). Electron micrograph confirmed that fine granular deposits in the first biopsy (asterisk G) disappeared in the third biopsy (H). Original magnification in A, B, C, D, E, F 400 ×; G 14000 ×; H 3500 ×.

tron microscopic examination confirmed complete resolution of the subendothelial fine granular deposits (Figure 1 G,H). The laboratory data obtained at the time of 2nd and 3rd biopsies are shown in Table 2.

Discussion

We found that high-dose chemotherapy with autologous PBSCT support ameliorated the nodular glomerular lesions characteristic of LCDD, which is thought to affect 3 – 5% of patients with underlying MM or other plasma cell dyscrasia [7, 8]. Since the early descriptions of LCDD by Randall et al. in 1976 [14], both patient and renal survival have been considered poor [4, 5, 13]: the median survival time of LCDD patients is reportedly 4.1 years, while the renal survival is 2.7 years [13]. The main prognostic factor for renal survival in LCDD is the degree of renal insufficiency, while those for patient survival are the degree of hematological disorder and extrarenal light chain deposition [13]. Several investigators have suggested that chemotherapy can stabilize or improve renal function in some LCDD patients who show mild-to-moderate renal insufficiency [4, 5, 10]. It has been unclear, however, whether such treatment can result in sustained remission. In addition, there has been only one report of the disappearance of nodular mesangial lesions after long-term conventional chemotherapy [10].

In recent years, high-dose chemotherapy with autologous PBSCT has emerged as a therapeutic option for treating patients with MM and AL-amyloidosis, even with renal in-

Table 2. Course of laboratory data.

	1st biopsy	2nd biopsy	3rd biopsy
Urinalysis			
Protein	4.8 g/day	0.34 g/day	0.0 g/day
Hematology			
Red blood cells	301 × 10^4 μl	222 × 10^4 μl	340 × 10^4 μl
Hemoglobin	9.6 g/dl	7.2 g/dl	11.8 g/dl
Hematocrit	28.4%	22.0%	33.9%
White blood cells	4,700/μl	4,600/μl	3,700/μl
Platelet	23.3 × 10^4 μl	7.9 × 10^4 μl	18.4 × 10^4 μl
ESR	100 mm/h	55 mm/h	38 mm/h
Chemistry			
Total protein	5.0 g/dl	5.9 g/dl	6.9 g/dl
Albumin	3.1 g/dl	3.7 g/dl	4.5 g/dl
Total cholesterol	223 mg/dl	255 mg/dl	239 mg/dl
Creatinine	1.5 mg/dl	0.9 mg/dl	1.0 mg/dl
Blood urea nitrogen	20 mg/dl	10 mg/dl	29 mg/dl
Uric acid	5.9 mg/dl	4.3 mg/dl	3.3 mg/dl
Sodium	149 mEq/l	147 mEq/l	139 mEq/l
Potassium	3.8 mEq/l	3.2 mEq/l	4.3 mEq/l
Chloride	114 mEq/l	108 mEq/l	104 mEq/l
Calcium	8.8 mg/dl	9.1 mg/dl	9.7 mg/dl
Phosphate	4.5 mg/dl	4.3 mg/dl	3.6 mg/dl
Serology			
CRP	0.5 mg/dl	0.1 mg/dl	0.2 mg/dl
IgG	297 mg/dl	1,153.2 mg/dl	918.6 mg/dl
IgA	40.4 mg/dl	90.2 mg/dl	214.2 mg/dl
IgM	10.8 mg/dl	74.8 mg/dl	39.7 mg/dl
M protein	(+)	(–)	(–)
BJP	(+)	(–)	(–)

volvement, and a favorable remission rate has been reported [2, 3, 16]. Royer et al. [15] reported that renal function and proteinuria were significantly improved after high-dose chemotherapy with autologous PBSCT. In addition, Lorenz and Hassoun et al. [6, 11] showed that autologous PBSCT may effectively provide long-term survival/renal function in patients with LCDD. However, histological resolution on renal biopsy was not confirmed in those reports. In our case of MM with LCDD, a renal biopsy 3 years after PBSCT showed reversal of the nodular glomerular lesions and disappearance of the light chain deposits.

Komatsuda et al. [10] reported that long-term suppression of the synthesis of abnormal κ light chain synthesis using conventional chemotherapy can lead to the disappearance of nodular glomerular lesions. This report suggests that it is necessary to control the production of free light chains for about 6 years to achieve resolution of the nodular glomerular lesions. In our case, however, 3 years of complete remission after high-dose chemotherapy with autologous PBSCT ameliorated the glomerular nodular lesions. Hassoun et al. [6] indicated that even low levels of circulating free light chains may have a deleterious effect on the kidneys. Light chains can induce the phenotypic changes in the cultured mesangial cells, which are characterized by the upregulation of tenascin-C and the inhibition of MMP-7 release. The end result may be the formation of nodules containing large quantities of tenascin-C [9]. Complete inhibition of light chain production using high-dose chemotherapy with autologous PBSCT may restore MMP-7 release from mesangial cells, which may in turn lead to the resolution of the glomerular nodular lesions.

As pointed out by the previous case report by Komatsuda et al. [10], chemotherapy may improve renal function in patients with a mild-to-moderate degree of renal insufficiency. The previous report by Lorenz et al. [11] indicated that a patient with a high serum creatinine (5.8 mg/dl) progressed to end-stage renal failure despite high-dose chemotherapy with autologous PBSCT. As renal insufficiency is mild in our case, we are uncertain as to wether or not high-dose chemotherapy with autologous PBSCT is applicable in patients with a high serum creatinine.

In conclusion, although earlier reports have shown that long-term chemotherapy can clear light chain deposits and restore renal function in cases of LCDD, this is the first report showing that, in the middle-term, high-dose chemotherapy with autologous PBSCT can ameliorate the glomerulosclerosis caused by LCDD and rescue renal function. Details of the mechanism underlying the pathogenesis of this glomerulosclerosis remain to be elucidated.

References

[1] *Buxbaum J, Gallo G.* Nonamyloidic monoclonal immunoglobulin deposition disease. Hematol Oncol Clin North Am. 1999; *13:* 1235-1248.

[2] *Casserly LF, Fadia A, Sanchorawala V et al.* High-dose intravenous melphalan with autologous stem cell transplantation in AL amyloidosis-associated end-stage renal disease. Kidney Int. 2003; *63:* 1051-1057.

[3] *Child JA, Morgan GJ, Davies FE et al.* Medical Research Council Adult Leukaemia Working Party. High-dose chemotherapy with hematopoietic stem-cell rescue for multiple myeloma. N Engl J Med. 2003; *348:* 1875-1883.

[4] *Ganeval D, Noël LH, Preud'homme JL, Droz D, Gruënfeld JP.* Light-chain deposition disease: Its relation with AL-type amyloidosis. Kidney Int. 1984; *26:* 1-9.

[5] *Heilman RL, Velosa JA, Holley KE, Offord KP, Kyle RA.* Long-term follow-up and response to chemotherapy in patients with light-chain deposition disease. Am J Kidney Dis. 1992; *20:* 34-41.

[6] *Hassoun H, Flombaum C, D'Agati VD et al.* High dose melphalan and auto-SCT in patients with monoclonal Ig deposition disease. Bone Marrow Transplant. 2008; *42:* 405-412.

[7] *Herrera GA, Joseph L, Gu X, Hough A, Barlogie B.* Renal pathologic spectrum in an autopsy series of patients with plasma cell dyscrasia. Arch Pathol Lab Med. 2004; *128:* 875-879.

[8] *Iványi B.* Frequency of light chain deposition nephropathy relative to renal amyloidosis and Bence Jones cast nephropathy in a necropsy study of patients with myeloma. Arch Pathol Lab Med. 1990; *114:* 986-987.

[9] *Keeling J, Herrera GA.* An in vitro model of light chain deposition disease. Kidney Int. 2009; *75:* 634-645.

[10] *Komatsuda A, Wakui H, Ohtani H et al.* Disappearance of nodular mesangial lesions in a patient with light chain nephropathy after long-term chemotherapy. Am J Kidney Dis. 2000; *35:* 9.

[11] *Lorenz EC , Gertz MA, Fervenza FC et al.* Long term outcome of autologous stem cell transplantation in light chain deposition disease. Nephrol Dial Transplant. 2008; *23:* 2052-2057.

[12] *Montseny JJ, Kleinknecht D, Meyrier A et al.* Long-term outcome according to renal histological lesions in 118 patients with monoclonal gammopathies. Nephrol Dial Transplant. 1998; *13:* 1438-1445.

[13] *Pozzi C, D'Amico M, Fogazzi GB et al.* Light chain deposition disease with renal involvemant: clinical characteristics and prognostic factors. Am J Kidney Dis. 2003; *42:* 1154-1163.

[14] *Randall RE, Williamson WC Jr, Mullinax F, Tung MY, Still WJ.* Manifestations of systemic light chain deposition. Am J Med. 1976; *60:* 293-299.

[15] *Royer B, Arnulf B, Martinez F et al.* High dose chemotherapy in light chain or light and heavy chain deposition disease. Kidney Int. 2004; *65:* 642-648.

[16] *Skinner M, Sanchorawala V, Seldin DC et al.* High-dose melphalan and autologous stem-cell transplantation in patients with AL amyloidosis: an 8-year study. Ann Intern Med. 2004; *140:* 85-93.

[Frontiers in Bioscience S2, 229-238, January 1, 2010]

EMT and TGF-beta in renal fibrosis

Masayuki Iwano

First Department of Internal Medicine, Nara Medical University, 840 Shijo, Kashihara, Nara 634-8522, Japan

TABLE OF CONTENTS

1. ABSTRACT

Transforming growth factor-beta1 (TGF-beta1) is a member of TGF-beta superfamily and the principal mediator contributing to the development and progression of renal fibrosis in a variety of disease settings. A critical effect of TGF-beta1 is the induction of epithelial-mesenchymal transition (EMT), which likely explains the continuous replenishment of fibroblasts during the progression of tissue fibrosis. Since we first identified EMT as the origin of fibroblasts in renal fibrosis, the signaling underlying EMT has been intensively studied in the field of nephrology. During the past five years, detailed mechanisms by which TGF-beta1 induces EMT have been clarified, and novel therapeutic approaches targeting TGF-beta1-mediated EMT are now being proposed.

2. INTRODUCTION

Epithelial-mesenchymal transition (EMT) is an important physiological event that occurs frequently during embryonic development (1). However, numerous reports have shown that EMT can also occur during pathological states, such as tumor metastasis and tissue fibrosis (2-6). It is well established that tissue fibroblasts are the principal effector cells in the accumulation of extracellular matrix (ECM), but the origin of those fibroblasts was not known until recently (7). Since our report that some fraction of the tissue fibroblasts involved in renal fibrosis originates from EMT, many studies have confirmed that EMT plays a critical role in the development and progression of renal fibrosis (4).

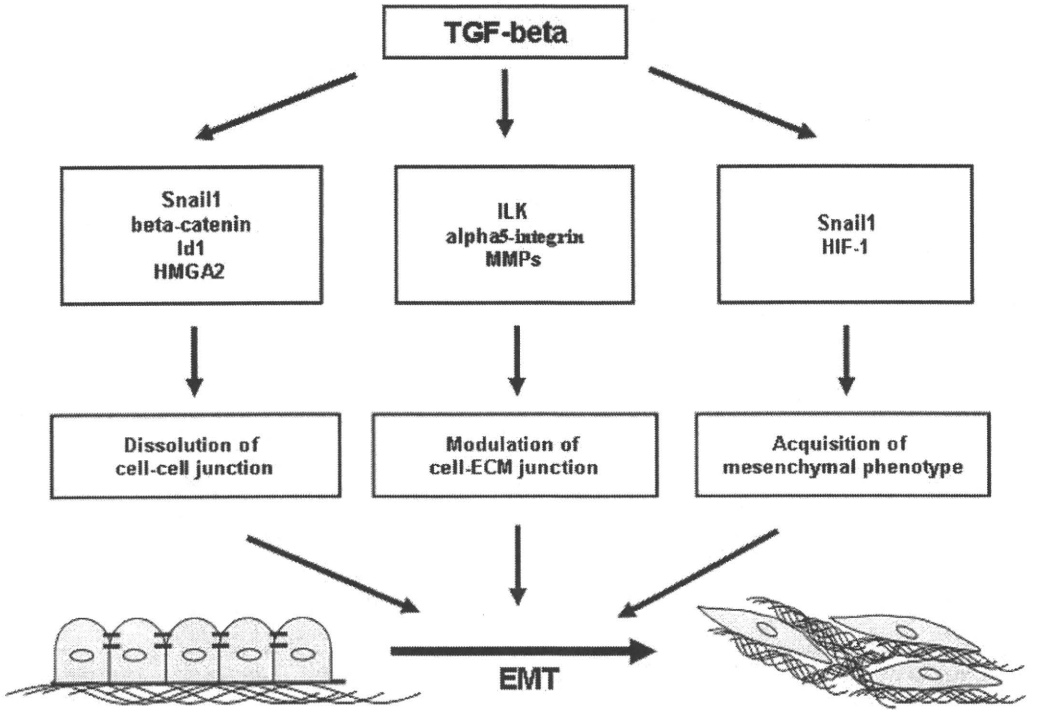

Figure 1. TGF-beta1 as a master regulator of EMT

EMT is a multi-step process involving the dissolution of tight junctions and adherens junctions, modulation of cell-ECM junctions, reorganization of the actin cytoskeleton, induction of mesenchymal gene expression, and acquisition of cellular motility. Numerous reports have shown that transforming growth factor-beta1 (TGF-beta1) is involved with these steps, and TGF-beta1 is now thought to be the master regulator governing the induction of EMT (8, 9) (Figure 1). Because epithelial cells are tightly bound to one another through cell-cell and cell-ECM junctions, dissolution of these junctions is necessary before epithelium can undergo EMT. Once epithelium looses its cellular polarity through the loss of these junctions, it acquires mesenchymal phenotypes, moves to interstitial areas, and participates in the accumulation of ECM. The mechanisms underlying this process are quite complex, and much remains to be learned about the molecular events mediating it. Identification of the key molecules (e.g., TGF-beta1) involved in the EMT process is essential for the development of novel therapies aimed at inhibiting the progression of fibrosis. In this review, we discuss the recent advances in our understanding of the biology of TGF-beta1-induced EMT, focusing on its role in renal fibrosis.

3. DISSOLUTION OF CELL-CELL ADHESION

E-cadherin is a well-known prototypical adhesion molecule localized in adherens junctions, which are linked to the cortical actin cytoskeletons of cells. Repression of E-cadherin is a hallmark of EMT and is considered to be an integral step in the EMT process. A variety of transcriptional factors, including Snail1, Slug (Snail2), SIP-1, ZEB-1, E12/E47 and Twist, are known to bind directly to E-boxes in the promoter regions of E-cadherin (8, 10, 11). In particular, studies have emphasized the key role played by the zinc-finger transcription factor Snail1 which TGF-beta1 has been shown to upregulate via both Smad-dependent and -independent signaling pathways (12-14). Madin-Darby canine kidney (MDCK) cells transfected with Snail1 show downregulated E-cadherin expression, increased expression of mesenchymal markers (vimentin and fibronectin), and transformation to a fibroblastoid phenotype (11). In transgenic mice, tamoxifen-induced Snail1 activation leads to development of renal fibrosis with the loss of epithelial features in renal tubules (15). Snail1 was also recently reported to be a critical regulator of fibroblast function *in vitro* and *in vivo*, and to continue to activate cellular motility and proliferation, even after terminal differentiation of mesenchymal cells (16).

Snail1 also binds directly to E-boxes in the promoter regions of two tight junction proteins, claudin and occludin, resulting in complete repression of their promoter activity. Snail1 is thus able to simultaneously repress expression of genes encoding both adherens and tight junctions (17). Claudin, occludin, two partitioning-defective proteins (PAR3 and PAR6) and zonula occludens (ZO)-1 are all membrane proteins localized at tight junctions, which are responsible for establishing and

maintaining epithelial cell polarity. Occludin binds to the TGF-beta type I receptor (TbetaRI) and promotes its recruitment to tight junctions. TGF-beta1-mediated induction of EMT is followed by the additional recruitment of TGF-beta type II receptor (TbetaRII) to the same junction complexes. In this way, occludin regulates TbetaRI localization for efficient TbetaRI-dependent dissolution of tight junctions during EMT (18). At the same time, Id1, an early TGF-beta1-inducible protein, suppresses expression of E-cadherin and ZO-1. Id1 also prevents HEB, a basic helix-loop-helix transcription factor, from binding to the E-box by sequestering it through formation of a heterodimeric HEB/Id1 complex, thereby blocking its transactivation of E-cadherin gene transcription (19).

Another molecule that has been shown to suppress E-cadherin gene transcription is T cell-specific transcription factor/lymphoid enhancer factor-1 (TCF/Lef1), which is associated with Wnt/beta-catenin signaling (13, 20). In renal proximal tubular cells, TGF-beta1-induced beta-catenin is required for synthesis of alpha-smooth muscle actin (alpha-SMA) as a marker of EMT (21). The Wnt signaling pathway is a necessary component that drives EMT in several embryonic processes (22). Wnt signaling promotes stabilization of cytoplasmic beta-catenin through phosphorylation of glycogen synthase kinase 3beta (GSK-3beta), which prevents beta-catenin's degradation (23). beta-Catenin is normally degraded via the ubiquitin proteosome pathway, which is mediated by a complex of proteins that includes adenomatous polyposis coli (APC), Axin and GSK-3beta (24). Dissociation of this complex as a result of GSK-3beta phosphorylation increases the stability of cytoplasmic beta-catenin and promotes its binding to TCF/Lef1. Subsequent nuclear translocation of the beta-catenin-TCF/Lef1 complex leads to a reduction in E-cadherin, thereby promoting EMT.

GSK-3beta phosphorylation has also been linked to the stable function of Snail1, which, like beta-catenin, is degraded via the ubiquitin pathway (25). Signaling pathways linked to phosphoinositide-3-kinase (PI3K) can also induce phosphorylation of GSK-3beta via downstream effectors such as integrin-linked kinase (ILK) and Akt (26). In addition, Snail1 and Slug promote formation of beta-catenin-TCF-4 transcription complexes that bind to the TGF-beta3 promoter to increase the gene's transcription. The resultant increase in TGF-beta3 signaling increases TCF/Lef1 gene expression, resulting in formation of beta-catenin-TCF/Lef1 complexes and thus initiation of EMT. Both TGF-beta1- and TGF-beta2-induced EMT appear to be TGF-beta3-dependent, establishing essential roles for multiple TGF-beta isoforms (27).

PAR3 and PAR6, two regulators of the apical-basal polarity of epithelial cells, were also reported to be key players during EMT. For instance, phosphorylation of PAR6 is required for TGF-beta1-dependent EMT in mammary gland epithelial cells. Ligand-activated TbetaRII phosphorylates PAR6, which in turn activates the E3 ubiquitin ligase SMURF1. SMURF1 then induces proteosomal degradation of RhoA, loss of the actomyosin ring and breakdown of apico-basal polarity (28). TGF-beta1 induces transcriptional downregulation of PAR3, resulting in the cytoplasmic localization of aPKC and PAR6, downregulation of E-cadherin and loss of tight and adherens junctions. Conversely, forced expression of PAR3 leads to a marked inhibition of TGF-beta1-induced E-cadherin suppression (29). Snail1 inhibits Crumbs-3 expression, leading to the relocalization of PALS1 and PATJ, two components of the Crumbs-3 complex, as well as the relocalization of the PAR complex, which is followed by loss of apica-basal polarity. Both the PAR and Crumbs polarity complexes are displaced from tight junctions in MDCK cells undergoing Snail1-induced EMT (30). At the same time, Twist, another Snail family transcription factor, and FTS-1-binding proteins engage their respective promoters. The net result is the emergence of the EMT proteome and repression of epithelial proteins. Loss of E-cadherins and cytokeratins, rearrangement of actin stress fibers and expression of fibroblast specific protein 1 (FSP1), vimentin, interstitial collagens and, occasionally, alpha-SMA, mark the morphological transition of epithelial cells into fibroblasts (31).

4. MODULATION OF CELL-ECM ADHESION

Renal fibrosis is characterized by excess accumulation of ECM in the interstitium. Tubular epithelial cells (TECs) are surrounded by ECM, so that their biological interaction likely plays a key role in the progression of renal fibrosis. Integrins are heterodimeric proteins comprised of alpha and beta subunits and serve as receptors for ECM proteins. In primary murine TECs, TGF-beta1 upregulates expression of alpha5-integrin, while knocking down alpha5-integrin attenuates TGF-beta1-mediated induction of mesenchymal markers like alphaSMA, suggesting integrin signaling is involved in the induction of the mesenchymal phenotype (32). The adaptor molecule disabled-2 (Dab2) is a positive mediator of TGF-beta1 signaling that acts by bridging the heteromeric TGF-beta1 receptor complex to Smad proteins. TGF-beta1 was recently reported to induce the transient accumulation of Dab2 at the membrane and to increase Dab2 binding to beta1 integrin, which occurs concomitantly with the promotion of EMT. Downregulation of Dab2 inhibits activation of integrin, as indicated by the reduction of TGF-beta1-induced phosphorylation of focal adhesion kinase and cellular adherence, leading to the inhibition of EMT (33).

TGF-beta1 induces Smad-dependent expression of ILK in TECs. ILK is an intracellular serine/threonine protein kinase that interacts with the cytoplasmic domains of beta-integrins and numerous other cytoskeleton-associated proteins. ILK is involved in the regulation of such integrin-mediated processes as cell adhesion, changes in cell shape and deposition of ECM. Forced expression of ILK in human proximal TECs suppresses E-cadherin and induces fibronectin and MMP-2, while expression of a dominant-negative ILK mutant abrogates TGF-beta1-initiated EMT, suggesting ILK plays a critical role in EMT (34). ILK also interacts with PINCH-1 (particularly interesting new cysteine-histidine rich protein-1), which

appears to be essential for its activity (35). However, selective ablation of ILK gene in TECs *in vivo* has not yet been done, and the function of ILK *in vivo* remains to be determined.

Dissolution of integrin-mediated cell-ECM adhesion by MMP2, MMP9 or MMP14 is also associated with the induction of renal tubular EMT. Disruption of the tubular basement membrane (TBM) is a complementary step in the initiation of EMT. As collagen type IV, the main constituent of the TBM, is a specific substrate of MMP-2 and MMP-9, it would seem likely these two enzymes are also involved in initiating EMT. Consistent with that idea, in the remnant kidney model, TGF-beta1 stimulates the synthesis of both MMP-2 and its activator protease, MMP-14, in TECs, after which these two enzymes colocalize at sites of basal lamina disruption (36).

5. EMT AND TGF-BETA1 SIGNALING

Because the majority of TGF-beta1 target genes are controlled via Smad-dependent pathways, Smads are thought to be essential for TGF-beta1-induced EMT. The binding of TGF-beta1 to TbetaRII causes the receptor to form a heterodimer with TbetaRI and to then phosphorylate TbetaRI. Phosphorylated TbetaRI then selectively recruits and phosphorylates R-Smad proteins (Smad2/3), which, when released from the receptor complex, oligomerize with Smad4. The resultant Smad2/3-Smad4 complex enters the nucleus to promote transcription of target genes (8, 9). TGF-beta1 induces Smad2/3 phosphorylation in a TEC line. Although both Smad2 and Smad3 are phosphorylated and activated by TbetaRI, they have strikingly different effects on gene transcription. Complexes of phosphorylated Smad2 and Smad4 have been shown to upregulate expression of TCF/Lef1, which can then associate with beta-catenin or reassociate with Smads to promote transcription of EMT target genes (37). Notably, however, selective ablation of Smad3 signaling inhibits renal fibrogenesis *in vivo* and blocks EMT *in vitro*, indicating that Smad2 signaling is dispensable for EMT and the progression of renal fibrosis (38). Moreover, deletion of Smad2 induces EMT in hepatocytes and keratinocytes, suggesting Smad2 is a negative regulator of Smad3 and acts to maintain the epithelial cell phenotype (39, 40). On the other hand, Snail1 expression is ablated in Smad3-null cells, suggesting Snail1-induced EMT is also dependent on Smad3 signaling (38). High mobility group A2 (HMGA2) binds directly to the Snail1 promoter and acts as a transcriptional regulator of Snail1 expression (41). HMGA2 is induced via the Smad pathway during EMT and recruits other transcriptional regulators, including Slug, Twist and Id2, all of which reportedly repress E-cadherin (42). The rapid induction of Id1 in human TECs after TGF-beta1 treatment is also dependent on Smad signaling (19).

Smad7 is an inhibitory Smad protein, overexpression of which markedly suppresses TGF-beta1-induced Smads2/3 activation, thereby preventing EMT and collagen synthesis (43, 44). Conversely, selective ablation of Smad7 accelerates the progression of renal fibrosis in a UUO model (45). Arcadia is an E3 ubiquitin ligase required for TGF-beta1 signaling during EMT. It stimulates EMT through degradation of Smad7, which suggests Smad signaling regulates EMT, both positively and negatively (46).

Gremlin, a bone morphogenic protein 7 (BMP-7) antagonist, is a downstream mediator of TGF-beta1, and has been shown to be upregulated in transdifferentiated renal proximal tubular cells and in human diabetic nephropathy, particularly in regions of tubulointerstitial fibrosis. Gremlin colocalizes with TGF-beta1, which is consistent with its importance as the effector of TGF-beta1-mediated EMT in renal fibrosis associated with human diabetic nephropathy (47, 48).

MicroRNA-155 is regulated via the TGF-beta1/Smads pathway and contributes to epithelial cell plasticity by targeting RhoA. TGF-beta1 induces microRNA-155 expression and promoter activity through Smad4. Knocking down microRNA-155 suppresses TGF-beta1-induced EMT and tight junction dissolution, while ectopic expression of microRNA-155 reduces levels of RhoA protein and disrupts tight junction formation (49). Conversely, the microRNA-200 family acts to prevent TGF-beta1-induced EMT (50). These associations between microRNAs and EMT have been investigated mainly in the context of cancer biology and not in renal fibrosis. Whether or not microRNA expression is associated with the EMT observed in renal fibrosis has not yet been determined.

Treatment of rat kidney epithelial cells (NRK52) with TGF-beta1 leads to activation of PI3K and Akt, as evidenced by increased phosphorylation of Ser473 of Akt and GSK-3beta, and by the observation that TGF-beta1-induced EMT phenotypes are blocked by inhibitors of PI3K and Akt (51). Thus TGF-beta1 also signals EMT in a Smad-independent manner. Indeed, in several systems TGF-beta1 signaling through Ras GTPase is required for EMT. What's more, TGF-beta1 receptors can signal through PAR6-SMURF1 to mediate ubiquitination of RhoA, an inhibitor of TGF-beta1-dependent EMT. In MDCKII cells, TGF-beta1 promotes EMT via the Smad-independent Ras-Raf-MEK-ERK-AP-1 signaling pathway, which upregulates Snail1 expression. Subsequent suppression of E-cadherin correlates with upregulation of mesenchymal markers (i.e., vimentin and fibronectin) and a definitive change in cellular morphology, but does not correlate with Smad signaling.

6. EMT IN THE GLOMERULUS

TGF-beta1 is also known to be an important mediator of glomerular damage, acting through the following mechanism. TGF-beta1 initially induces EMT in glomerular epithelial cells (podocytes). Exposing immortalized mouse podocytes to TGF-beta1 suppresses expression of P-cadherin, ZO-1 and nephrin, while inducing expression of desmin, fibronectin and collagen type I. Ectopic expression of Snail1 also suppresses P-cadherin and nephrin in podocytes, which, given that TGF-

beta1 induces Snail1 (see above), suggests TGF-beta1 has the capacity to mediate EMT in podocytes. Consistent with these *in vitro* data, loss of epithelial markers (nephrin and ZO-1) by podocytes and gain of mesenchymal markers (desmin, FSP1 and MMP9) are also observed in human diabetic nephropathy (52). EMT can lead to the detachment of podocytes from the glomerular basement membrane, which in turn leads to glomerular sclerosis. TGF-beta1 is also associated with the subsequent formation of cellular crescents, within which expression of ILK is strongly induced. ILK-expressing cells within cellular crescents are also positive for protein gene product 9.5 (parietal epithelial cell marker), alphaSMA and TGF-beta1, suggesting TGF-beta1-mediated upregulation of ILK expression contributes to the induction of EMT in parietal epithelial cells, which in turn appears to contribute to the further formation of cellular crescents and global glomerular damage (53). Finally, TGFbeta1 induces mesangial accumulation of ECM by accelerating mesangial cell fibrogenesis (54).

The progression of kidney disease is more closely associated with tubulointerstitial fibrosis than with glomerular injury (55). The link between glomerular disease and tubulointerstitial fibrosis likely involves an interstitial microvascular circulation that is compromised by upstream glomerular disease. The obliteration of postglomerular capillaries as a result of glomerular sclerosis or severe glomerular injury due to crescent formation impairs peritubular perfusion because the glomerular efferent arterioles branch into the peritubular capillary networks surrounding the tubular segments. The resultant peritubular capillary loss or low blood flow reduces the oxygen supply to the interstitium, leading to chronic interstitial and tubular cell hypoxia, which can initiate and sustain interstitial scarring and tubular atrophy. We recently showed that stable expression of hypoxia inducible factor-1 (HIF-1) by TECs in a hypoxic state promotes renal fibrosis and that HIF-1 is essential for induction of EMT in TECs (56-58). HIF-1 induces activation of cellular motility through upregulation of lysyl oxidase genes (56). Moreover, recent studies indicate that TGF-beta1 increases the expression of the regulatory HIF-1alpha subunit and the binding of HIF-1 to DNA. TGF-beta1 stimulates HIF-1 accumulation and activity by increasing the stability of the HIF-1alpha subunit (59). In addition, hypoxia and TGF-beta1 act synergistically to enhance production of certain types of collagen in fibroblasts (60). Although the molecular basis of the functional interaction is not well understood, such crosstalk between HIF-1 and TGF-beta1 may play a key role in the progression of renal fibrosis.

7. NEW THERAPEUTIC STRATEGIES AIMED AT INHIBITING TGF-BETA1-INDUCED EMT

Although EMT is an important element of the pathophysiology underlying the progression of renal fibrosis, there are at present no therapies aimed at preventing EMT as a means of treating chronic kidney disease in humans. Hepatocyte growth factor (HGF) and BMP-7 are well-known EMT antagonists. HGF binds to its c-Met tyrosine kinase receptor and engages STAT3 during the formation of epithelial tubules. It also upregulates the expression of the Smad transcriptional co-repressor SnoN in tubular epithelial cells and negatively regulates EMT by interfering with Smad2/3 signaling. These inhibitory effects of HGF on EMT retard renal fibrogenesis in mice (61, 62).

In several models of kidney injury, administration of BMP-7 attenuates renal fibrogenesis while restoring the structure of tubular epithelial units (63). BMP-7 induces mesenchymal-epithelial transition (MET) by utilizing another set of Smads (Smad1/5), and reverses the EMT phenotype driven by TGF-beta1 (64). Although the precise mechanism and signaling pathways via which MET occurs remain unknown, a full understanding of this reciprocal phenomenon could form the basis for potentially highly effective novel therapeutic strategies. In a recent report, however, attenuation of TGF-beta1-induced EMT and corresponding induction of MET by BMP-7 could not be confirmed in human proximal TECs (65).

Treatment with BMP-2 also reverses the TGF-beta1-induced increase in fibronectin concomitantly with a significant downregulation of TbetaRI. BMP-2 shortens the half-life of TbetaRI through an effect on the ubiquitin proteosome degradation pathway, and reverses the TGF-beta1-induced increase in pSmad2/3, as well as the TGF-beta1-induced downregulation of inhibitory Smad7 (66). Interestingly, latent TGF-beta1 seems to protect against renal inflammation in a model of ureteral obstruction. In transgenic mice, overexpression of latent TGF-beta1 in keratinocytes reduced proteinuria by 50%, suppressed the formation of glomerular crescents by 70%, thereby preserving renal function (67). Progressive renal fibrosis was also prevented in these mice, and the protective effects were associated with elevated levels of latent, but not active, TGF-beta1 in plasma and renal tissue (68).

C-peptide reportedly interrupts TGF-beta1 signaling pathways and blocks development of EMT in HK2 human kidney proximal tubular cells. EMT-associated morphological alteration of proximal tubular cells, including increased vimentin expression, reduced E-cadherin expression, and cytoskeletal rearrangements can be prevented by treatment with C-peptide. C-peptide also blocks TGF-beta1-induced upregulation of expression of both TbetaRI and TbetaRII, and attenuates TGF-beta1-mediated Smad phosphorylation and Smad transcriptional activity. Thus C-peptide almost completely reverses the morphological changes induced by TGF-beta1 in proximal tubular cells, which suggests that it could serve as a renoprotective agent in diabetic nephropathy (69). If the results of clinical trials are promising, BMP-2, BMP-7, HGF, latent TGF-beta1 or C-peptide could become an important new adjuvant in the pharmacological armamentarium used to treat fibrogenesis.

GW 788388 is a new TbetaRI inhibitor that blocks TGF-beta1-induced Smad activation and target gene expression while reducing EMT and fibrosis. For instance, GW788388 given orally for 5 weeks reduced renal fibrosis

as well as the expression of key mediators of ECM in the kidneys of db/db mice (70). In addition, inhibition of histone deacetylase 6 (HDAC6) attenuated TGF-beta1-induced EMT, in part because reducing HDAC6 expression impairs the activation of Smad3 – e.g., the HDAC inhibitor trichostatin A prevented TGF-beta1-induced EMT in human TECs (71). At present, several clinical trials are investigating the effects of anti-TGF-beta1 antibodies in diabetic nephropathy. It is hoped that anti-TGF-beta1 therapy will become an important new tool to add to ACEI/ARB therapy for the treatment of human kidney diseases (72).

Heat shock proteins (HSPs) are the main effectors of cellular repair, and the association between EMT and HSP expression in renal fibrosis has been analyzed. HSP47, a collagen-specific molecular chaperone, is a surrogate marker of collagen synthesis and assists in the assembly of procollagen. HSP47 colocalizes with FSP1 in the renal fibrosis observed in human IgA nephropathy, suggesting it is involved in the accumulation of collagen (73). Consistent with that idea, *in vivo* administration of HSP47 siRNA in the UUO model diminished the interstitial fibrosis (74). In addition, although TGF-beta1 upregulates the levels of total and phosphorylated HSP27, HSP27 protects E-cadherin expression and blocks EMT by downregulating Snail1 expression (75). HSP27 may be induced in renal fibrosis through a negative feedback loop affecting EMT. In TECs, TGF-beta1-induced EMT is also inhibited by selective expression of HSP72. Moreover, in the UUO model, oral administration of geranylgaranylacetone, a selective inducer of HSP72, significantly diminished the progression of renal fibrosis (76).

Early treatment of anemia using recombinant human erythropoietin (rhEPO) has also proven effective for the treatment of chronic renal failure. EPO is thought to exert several pleiotropic effects. rhEPO treatment reduced levels of TGF-beta1, alphaSMA and fibronectin expression, and inhibited the progression of renal fibrosis in the UUO model. The increased alphaSMA and vimentin expression and decreased E-cadherin expression caused by TGF-beta1 in MDCK cells was attenuated by co-administration of rhEPO, indicating the renoprotective effects of rhEPO may be mediated by inhibition of TGF-beta1-induced EMT (77).

Several reports have shown that vitamin D analogues are renoprotective in experimental animal models of chronic kidney diseases. A clinical trial also demonstrated the antiproteinuric effects of oral paricalcitol, a synthetic vitamin D analogue, in chronic kidney disease. Paricalcitol is able to target the EMT process through preservation of E-cadherin and inhibition of EMT markers, and *in vivo* paricalcitol suppresses renal expression of both TbetaRI and Snail1 (78). Finally, rapamycin and mycophenolate mofetil (MMF) have a greater inhibitory effect on EMT *in vitro* than older immunosuppresives and may result in less fibrosis and a better long-term allograft survival (79). Thus, exploration of the drugs available for the treatment of chronic kidney disease is yet another treatment option.

8. CONCLUSIONS

More than 40% of all deaths in developed countries are attributable to chronic fibrosis, including renal fibrosis, liver cirrhosis, pulmonary fibrosis and cardiovascular fibrosis. Consequently, the search for antifibrotic drugs is a challenging and highly important project. TGF-beta1 is the pivotal factor controlling the progression of tissue fibrosis, but data on the clinical application of anti-TGF-beta1 therapy remains limited. Because tissue fibrosis is a kind of physiological adaptation to prevent expansion of areas of inflammation, thereby protecting organs from functional deterioration, controlling fibrosis in way that is beneficial to the body is not simple. However, recent advances in EMT biology should provide a variety of tools for establishing novel therapeutic approaches to the treatment of tissue fibrosis. For instance, it is possible that the combination of EMT inhibitors with conventional RAAS inhibition could improve renal survival in chronic kidney disease. And a method for inducing MET and the recovery from progressive fibrosis would be of incalculable clinical value and a landmark advance in the medical sciences.

9. ACKNOWLEDGMENTS

This work was supported in part by research grant 19590960 from the Ministry of Education and Science of Japan and Grants-in-Aid for the Research Group on Progressive Renal Diseases from the Ministry of Health, Labor, and Welfare of Japan.

10. REFERENCES

1. E.D. Hay: An overview of epithelio-mesenchymal transformation. *Acta Anat (Basel)* 154, 8-20 (1995)

2. J.P. Thiery: Epithelial-mesenchymal transitions in tumour progression. *Nat Rev Cancer* 2, 442-454 (2002)

3. M. Iwano and E.G. Neilson: Mechanisms of tubulointerstitial fibrosis. *Curr Opin Nephrol Hypertens* 13, 279-284 (2004)

4. M. Iwano, D. Plieth, T.M. Danoff, C. Xue, H. Okada and E.G. Neilson: Evidence that fibroblasts derive from epithelium during tissue fibrosis. *J Clin Invest* 110, 341-350 (2002)

5. E.G. Neilson: Setting a trap for tissue fibrosis. *Nat Med* 11, 373-374 (2005)

6. R. Kalluri and E.G. Neilson: Epithelial-mesenchymal transition and its implications for fibrosis. *J Clin Invest* 112, 1776-1784 (2003)

7. M. Iwano, A. Fischer, H. Okada, D. Plieth, C. Xue, T.M. Danoff and E.G. Neilson: Conditional abatement of tissue fibrosis using nucleoside analogs to selectively corrupt DNA replication in transgenic fibroblasts. *Mol Ther* 3, 149-159 (2001)

8. J. Zavadil and E.P. Bottinger: TGF-beta and epithelial-

to-mesenchymal transitions. *Oncogene* 24, 5764-5774 (2005)

9. J. Xu, S. Lamouille and R. Derynck : TGF-beta-induced epithelial to mesenchymal transition. *Cell Res* 19, 156-172 (2009)

10. E. Batlle, E. Sancho, C. Franci, D. Dominquez, M. Monfar, J. Baulida and D.H.A. Garcia: The transcriptional factor snail is a repressor of E-cadherin gene expression in epithelial tumour cells. *Nat Cell Biol* 2, 84-89 (2000)

11. A. Cano, M.A. Perez-Moreno, I Rodrigo, A. Locascio, M.J. Blanco, M.G. del Barrio, F. Portillo and M.A. Nieto: The transcription factor snail controls epithelial-mesenchymal transitions by repressing E-cadherin expression. *Nat Cell Biol* 2, 76-83 (2000)

12. H. Peinado, M. Quintanilla and A. Cano: Transforming growth factor beta1 induces snail transcription factor in epithelial cell line: mechanisms for epithelial mesenchymal transitions. *J Biol Chem* 278, 21113-21123 (2003)

13. D. Medici, E.D. Hay and D.A. Goodenough: Cooperation between snail and LEF-1 transcription factors is essential for TGF-beta1-induced epithelial-mesenchymal transition. *Mol Biol Cell* 17, 1871-1879 (2006)

14. H.J. Cho, K.E. Baek, S. Saika, M.J. Jeong and J. Yoo: Snail is required for transforming growth factor-beta-induced epithelial-mesenchymal transition by activating PI3 kinase/Akt signal pathway. *Biochem Biophys Res Commun* 353, 337-343 (2007)

15. A. Boutet, C.A. De Frutos, P.H. Maxwell, M.J. Mayol, J. Romero and M.A. Nieto: Snail activation disrupts tissue homeostasis and induces fibrosis in the adult kidney. *EMBO J* 25, 5603-5613 (2006)

16. R.G. Rowe, X.Y. Li, Y. Hu, T.L. Saunders, I Virtanen, A. Garcia de Herreros, K.F. Becker, S. Ingvarsen, L.H. Engelholm, G.T. Bommer, E.R. Fearon and S.J. Weiss: Mesenchymal cells reactivate Snail1 expression to drive three-dimentional invasion programs. *J Cell Biol* 184, 399-408 (2009)

17. J. Ikenouchi, M Matsuda, M. Furuse and S. Tsukita: Regulation of tight junctions during the epithelium-mesenchyme transition: direct repression of the gene expression of claudins/occludin by Snail. *J Cell Sci* 116, 1959-1967 (2003)

18. M. Barrios-Rodiles, K.R. Brown, B. Ozdamar, R. Bose, Z. Liu, R.S. Donovan, F. Shinjo, Y. Liu, J. Dembowy, I.W. Taylor, V. Luga, N. Przulj, M. Robinson, H. Suzuki, Y. Hayashizaki, I. Jurisica and J.L. Wrana: High-throughput mapping of a dynamic signaling network in mammalian cells. *Science* 307, 1621-1625 (2005)

19. Y. Li, J. Yang, J.H. Luo, S. Dedhar and Y. Liu: Tubular epithelial cell dedifferentiation is driven by the helix-loop-helix transcriptional inhibitor Id1. *J Am Soc Nephrol* 18, 449-460 (2007)

20. M. Reichert, T. Muller and W. Hunziker: The PDZ domains of zonula occludens-1 induce an epithelial to mesenchymal transition of Madin-Darby canine kidney I cells. Evidence for a role of beta-ccatenin/Tcf/Lef signaling. *J Biol Chem* 275, 9492-9500 (2000)

21. A. Masszi, L. Fan, L. Rosivall, C.A. McCulloch, O.D. Rotstein, I. Mucsi and A. Kapus: Integrity of cell-cell contacts is a critical regulator of TGF-beta1-induced epithelial-to-myofibroblast transition. *Am J Pathol* 165, 1955-1967 (2004)

22. A. Nawshad, D. Laqamba, A. Polad and E.D. Hay: Tranforming growth factor-beta signaling during epithelial-mesenchymal transformation: implication for embryogenesis and tumor metastasis. *Cells Tissues Organs* 179, 11-23 (2005)

23. S. Ikeda, S. Kishida, H. Yamamoto, H. Murai, S. Koyama and A. Kikuchi: Axin, a negative regulator of the Wnt signaling pathway, forms a complex with GSK-3beta and beta-catenin and promotes GSK-3beta-dependent phosphorylation of beta-catenin. *EMBO J* 17, 1371-1384 (1998)

24. N.C. Ha, T. Tonozuka, J.L. Stamos, H.J. Choi and W.I. Weis: Mechanism of phosphorylation-dependent binding of APC to beta-catenin and its role in beta-catenin degradation. *Mol Cell* 15, 511-521 (2004)

25. B.P. Zhou, J. Deng, W. Xia, J. Xu, Y.M. Li, M. Gunduz and M.C. Hung: Dual regulation of Snail by GSK-3beta-mediated phosphorylation in control of epithelial-mesenchymal transition. *Nat Cell Biol* 6, 931-940 (2004)

26. M. Delcommenne, C. Tan, V. Gray, L. Rue, J. Woodqett and S. Dedhar: Phosphoinositide-3-OH kinase-dependent regulation of glycogen synthase kinase 3 and protein kinase B/AKT by the integrin-linked kinase. *Proc Natl Acad Sci USA* 95, 11211-11216 (1998)

27. D. medici, E.D. Hay and B.R. Olsen: Snail and Slug promote epithelial-mesenchymal transition through beta-catenin-T-cell factor-4-dependent expression of transforming growth factor-beta3. *Mol Biol Cell* 19, 4875-4887 (2008)

28. B. Ozdamar, R. Bose, M. Barrios-Rodiles, H.R. Wang, Y. Zhang and J.L. Wrana: Regulation of the polarity protein Par6 by TGFbeta receptors controls epithelial cell plasticity. *Science* 307, 1603-1609 (2005)

29. X. Wang, J. Nie, Q. Zhou, W. Liu, F. Zhu, W. Chen, H. Mao, N. Luo, X. Dong and X. Yu: Downregulation of Par-3 expression and disruption of Par complex integrity by TGF-beta during the process of epithelial to mesenchymal transition in rat proximal epithelial cells. *Biochim Biophys Acta* 1782, 51-59 (2008)

30. E.L. Whiteman, C.J. Liu, E.R. Fearon and B. Marqolis: